

Cation–Cation Interactions and Antiferromagnetism in Na[Np(V)O₂(OH)₂]: Synthesis, Structure, and Magnetic Properties

Philip M. Almond,^{†,‡} S. Skanthakumar,[†] L. Soderholm,^{*,†,‡} and Peter C. Burns^{*,†,‡}

Chemistry Division, Argonne National Laboratory, Argonne, Illinois 60439, and Department of Civil Engineering and Geosciences, University of Notre Dame, South Bend, Indiana 46556

Received September 5, 2006. Revised Manuscript Received November 4, 2006

Na[NpO₂(OH)₂] (**1**) crystallizes from the hydrothermal reaction of Np(V) and NaOH, in an aqueous solution with a pH of 14, over 3 days at 120 °C. The single-crystal X-ray structure was solved by direct methods and refined via full-matrix least-squares on F^2 . The compound crystallizes in the orthorhombic space group $P2_12_12_1$, $a = 5.8904(3)$ Å, $b = 7.6297(4)$ Å, $c = 8.1540(4)$ Å, $Z = 4$, with $R(F) = 1.52\%$, $wR2(F^2) = 3.51\%$ obtained using 63 refined parameters and 1400 reflections. The three-dimensional structure is built from (Np(V)O₂)O(OH)₄ pentagonal bipyramids that are linked through bridging hydroxyl groups to form a one-dimensional chain substructure, analogous to chains observed in the U(VI) phases of moctezumite, [PbUO₂(TeO₃)₂], and (UO₂)Cl₂(H₂O). Each chain extends along the b -axis and is rotated approximately 60° from neighboring chains, thus permitting the bonding of a dioxo ligand on a neptunyl in one chain as an equatorial ligand of a neighboring NpO₂⁺ ion in an adjacent chain. This unusual bonding configuration, known as a cation–cation interaction, fuses the neptunyl chains into a three-dimensional framework that contains small orthogonally intersecting channels, which contain the Na⁺ cations. The magnetic response of **1** as a function of applied field and temperature is consistent with an antiferromagnetic ordering of Np moments below 19.5(5) K. The effective moment determined over the temperature range of 35–300 K is 2.80(15) μ_B per formula unit.

Introduction

Generated in nuclear reactors, and considered problematic for long-term waste disposal, ²³⁷Np (neptunium, atomic number 93, $t_{1/2} = 2.14 \times 10^6$ years) has received increased attention in recent years about its crystal chemistry,^{1–6} magnetic properties,^{7–11} and environmental impact.^{3,12,13} Despite these recent reports, relatively little is known about the chemistry of this redox-active ion under environmentally

relevant conditions. The pentavalent oxidation state occurs as the linear dioxo neptunyl(V) cation [O=Np=O]⁺ in solution, similar in coordination to that seen for hexavalent uranium.

In contrast to the extensive knowledge that has been developed for uranyl solid-state chemistry,¹⁴ there is relatively little known about the corresponding crystal chemistry for neptunyl, in large part the result of the lack of a geological basis from which to work. There is a tendency to assume that the structural chemistry of uranyl(VI) can serve as a model for neptunyl systems. Whereas this appears to be a valid approach for neptunyl(VI), this approach does not appear adequate for Np(V) crystal chemistry, which is expected to dominate environmentally germane systems. In addition to compensating for the difference in charge between uranyl(VI) and neptunyl(V), the latter ion also has a propensity for the dioxo ligands associated with one neptunyl to bind as equatorial ligands on an adjacent neptunyl.¹⁵ First hypothesized to explain results in solution and labeled “cation–cation interactions”,¹⁶ this additional bonding by the dioxo ligands is seen in approximately 30% of the Np(V) structures but remains rare in uranyl chemistry^{14,17,18}

The difference in cation–cation bonding preference between uranyl(VI) and neptunyl(V) presumably arises because

* Corresponding authors. E-mail: LS@ANL.gov (L.S.); pburns@nd.edu (P.C.B.).

[†] Argonne National Laboratory.

[‡] University of Notre Dame.

- (1) Charushnikova, I. A.; Krot, N. N.; Polyakova, I. N. *Radiochemistry (New York)* **2006**, *48*, 1–5.
- (2) Grigor'ev, M. S.; Fedoseev, A. M.; Budantseva, N. A.; Antipin, M. Y. *Radiochemistry (New York)* **2005**, *47*, 545–548.
- (3) Forbes, T. Z.; Burns, P. C. *J. Solid State Chem.* **2005**, *178*, 3445–3452.
- (4) Andreev, G. B.; Antipin, M. Y.; Budantseva, N. A.; Krot, N. N. *Russ. J. Coord. Chem.* **2005**, *31*, 800–803.
- (5) Tian, G.; Xu, J.; Rao, L. *Angew. Chem., Int. Ed.* **2005**, *44*, 6200–6203.
- (6) Charushnikova, I. A.; Fedoseev, A. M.; Starikova, Z. A. *Russ. J. Coord. Chem.* **2005**, *31*, 603–607.
- (7) Forbes, T. Z.; Burns, P. C.; Soderholm, L.; Skanthakumar, S. *Chem. Mater.* **2006**, *18*, 1643–1649.
- (8) Almond, P. M.; Sykora, R. E.; Skanthakumar, S.; Soderholm, L.; Albrecht-Schmitt, T. E. *Inorg. Chem.* **2004**, *43*, 958–963.
- (9) Joblionic, E.; Oshima, Y.; Brooks, J. S.; Albrecht-Schmitt, T. E. *Solid State Commun.* **2004**, *132*, 337–342.
- (10) Nakamoto, T.; Nakada, M.; Nakamura, A. *J. Nucl. Sci. Technol.* **2002**, *Suppl. 3*, 102–105.
- (11) Nakamoto, T.; Masami, N.; Nakamura, A. *Solid State Commun.* **2001**, *119*, 523–526.
- (12) Burns, P. C.; Deely, K. M.; Skanthakumar, S. *Radiochim. Acta* **2004**, *92*, 151–159.
- (13) Kaszuba, J. P.; Runde, W. H. *Environ. Sci. Technol.* **1999**, *33*, 4427–4433.

(14) Burns, P. C. *Can. Mineral.* **2005**, *43*, 1839–1894.

(15) Krot, N. N.; Grigor'ev, M. S. *Russ. Chem. Rev.* **2004**, *73*, 89–100.

(16) Sullivan, J. C.; Hindman, J. C.; Zielen, A. J. *J. Am. Chem. Soc.* **1961**, *83*, 3373–3378.

(17) Sullens, T. A.; Jensen, R. A.; Shvareva, T. Y.; Albrecht-Schmitt, T. E. *J. Am. Chem. Soc.* **2004**, *126*, 2676–2677.

(18) Li, Y.; Cahill, C. L.; Burns, P. C. *Chem. Mater.* **2001**, *13*, 4026–4031.

the bonding requirements of the dioxo ligands in the former case are met by bonding to U alone, whereas for the latter case the bond valence of the dioxo ligands bonded only to Np(V) is considerably less than 2,¹⁹ thus stabilizing structures in which the oxo ligands have additional bonding opportunities.

The occurrence of cation–cation interactions in Np(V) compounds, which have an f² configuration, provides an opportunity for enhanced magnetic interactions. The Np–Np distances reported for cation–cation interactions cover a range of approximately 3.48–4.24 Å¹⁵ with an average distance of about 4.1 Å.⁷ The magnetic response of a limited number of these compounds has been studied,^{7,8,11,20–22} and all show evidence of ferromagnetic ordering in the range of 8–12 K. Ferromagnetic ordering in molecular oxides is somewhat unusual; its dominance among these Np(V) compounds may reflect either the symmetry of the coupling or the distance between Np centers.

In this article we report the synthesis, structure, and magnetic properties of Na[NpO₂(OH)₂] (**1**). This compound contains one crystallographic Np(V) that is linked to other Np through both hydroxyl bridges and cation–cation interactions. A comparison of **1** with UO₂²⁺ oxide hydrate phases is presented in order to emphasize the effects of cation–cation interactions on structure.

Experimental Section

Synthesis. A 90 mM stock solution of ²³⁷NpO₂⁺ in 1 M HCl and a 2 M solution of NaOH (95%, Fisher) were prepared using Millipore filtered water with a resistance of 17.4 MΩ. **Caution:** ²³⁷Np represents a serious health risk due to the emission of α- and γ-radiation. Such studies require appropriate infrastructure and personnel trained in the handling of radioactive materials. Na[NpO₂(OH)₂] (**1**): A volume of 470 μL of the stock solution containing 90 mM ²³⁷NpO₂⁺ in 1 M HCl was added to a 7 mL Teflon screw cap vial followed by the addition of 1 mL of a 2 M NaOH solution to give a pH of 14. The vial was sealed and subsequently loaded into a 125 mL PTFE-lined autoclave prefilled with 50 mL of water. The autoclave was sealed and placed in a box furnace preheated to 120 °C. After 72 h, the furnace was slowly cooled over 10 h to 23 °C. The product consisted of a clear, colorless solution over transparent magenta needles of **1**. The crystals were washed with ethanol and allowed to dry. A pure yield was confirmed via comparison of powder diffraction patterns of **1** to its calculated diffraction pattern derived from the single-crystal data. The final measured pH of the mother liquor was 14. The addition of hydrogen peroxide to the reactants allowed for the isolation of larger crystals of **1** along with an unidentified powder.

Crystallographic Studies. A single crystal of **1** measuring 0.081 mm × 0.012 mm × 0.011 mm was mounted on a glass fiber and optically aligned on a Bruker APEX-II CCD X-ray diffractometer using APEX-II (v 1.0-22) software.²³ A sphere of three-dimensional data was collected using graphite-monochromated Mo Kα radiation

Table 1. Crystallographic Data for Na[NpO₂(OH)₂] (**1**)

structure formula	Na[NpO ₂ (OH) ₂]
formula weight	326.01
temp (K)	298
wavelength (Å)	0.71073
space group	P2 ₁ 2 ₁ 2 ₁ (No. 19)
<i>a</i> (Å)	5.8904(3)
<i>b</i> (Å)	7.6297(4)
<i>c</i> (Å)	8.1540(4)
vol (Å ³)	366.46(3)
Z	4
density (g/cm ³)	5.909
μ (mm ⁻¹)	28.321
<i>F</i> (000)	552
cryst size (mm)	0.081 × 0.012 × 0.011
theta range for data collection (deg)	3.66–33.48
limiting indices	−8 < <i>h</i> < 9, −11 < <i>k</i> < 11, −12 < <i>l</i> < 12
reflns collected/unique	6586/1400
refinement method	full-matrix least-squares on <i>F</i> ²
data/restraints/params	1400/0/63
goodness-of-fit on <i>F</i> ²	1.041
final <i>R</i> indices [<i>I</i> > 2σ(<i>I</i>)]	<i>R</i> 1 = 0.0152, <i>wR</i> 2 = 0.0349
<i>R</i> indices (all data)	<i>R</i> 1 = 0.0161, <i>wR</i> 2 = 0.0351
largest diff peak and hole (Å ³)	2.387 and −0.989

from a sealed tube and monocapillary collimator. Data collection included four unique series of exposures of 600 frames with an exposure time of 30 s per frame and frame widths of 0.3° in ω.

The determination of corrected integrated intensities and global refinement of lattice parameters were performed using SAINT+ (v 7.09) with a narrow-frame integration algorithm.²⁴ A semiempirical absorption correction was subsequently applied with the program SADABS.²⁵ SHELXTL (v 6.14) software was used for space group determination (XPREP), direct methods structure solution (XS), and least-squares refinement (XL).²⁶ The orthorhombic chiral space group P2₁2₁2₁ was indicated by systematic absences. The structure was solved via direct methods and refined by full-matrix least-squares on the basis of *F*². The final refinement included anisotropic displacement parameters for all non-hydrogen atoms. Hydrogen atoms were located in the difference maps and were included in the refinement. Selected crystallographic details are given in Table 1. Further details may be found in the Supporting Information.

Magnetic Measurements. The magnetic behavior of Na[NpO₂(OH)₂] was measured using a superconducting quantum interference device (SQUID) magnetometer, over the temperature range of 5–320 K. Due to the radiological hazards associated with ²³⁷Np, the sample was double-encapsulated in a sealed aluminum holder that contributed considerably (up to 90%) to the measured signals. Susceptibility data was acquired for three polycrystalline samples under an applied field of 500 and 2000 G. Linearity of the *M* versus *H* responses was confirmed at 50 K for the higher field. In addition, the sample was examined for evidence of long-range magnetic order by taking temperature-dependent measurements at several fields, as low as 20 G, over the temperature range of 5–20 K. Hysteresis measurements were also recorded at 5 K to fields as high as 25 000 G. Empty Al sample holders were measured separately under identical conditions, and their magnetic response was subtracted directly from the raw data. The measured susceptibility data was further corrected by removing the diamagnetic contribution of the sample from the raw data.

Results and Discussion

Structure Description. Na[NpO₂(OH)₂] (**1**). The structure of Na[NpO₂(OH)₂] contains a single symmetrically distinct

(19) Burns, P. C.; Ewing, R. C.; Miller, M. L. *J. Nucl. Mater.* **1997**, *245*, 1–9.

(20) Albrecht-Schmitt, T. E.; Almond, P. M.; Sykora, R. E. *Inorg. Chem.* **2003**, *42*, 3788–3795.

(21) Cousson, A.; Dabos, S.; Abazli, H.; Nectoux, F.; Pages, M.; Choppin, G. *J. Less-Common Met.* **1984**, *99*, 233–240.

(22) Nakamoto, T.; Nakada, M.; Nakamura, A.; Haga, H.; Onuki, Y. *Solid State Commun.* **1999**, *109*, 77–81.

(23) Bruker. *APEX-II*; Bruker AXS, Inc.: Madison, WI, 2004.

(24) Bruker. *SAINT+*; Bruker AXS, Inc.: Madison, WI, 2004.

(25) Sheldrick, G. M. *SADABS*; University of Göttingen: Göttingen, Germany, 2004.

(26) Sheldrick, G. M. *SHELXTL*; Bruker AXS Inc.: Madison, WI, 1997.

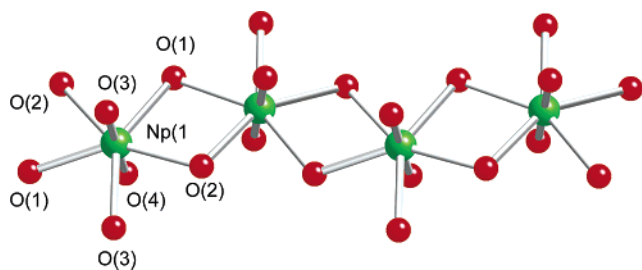


Figure 1. Depiction of the one-dimensional neptunyl hydroxide chain excised from the three-dimensional structure of $\text{Na}[\text{NpO}_2(\text{OH})_2]$. These chains are built from edge-sharing $(\text{NpO}_2)\text{O}(\text{OH})_4$ pentagonal bipyramids that link through bridging hydroxyl anions and extend along the b -direction.

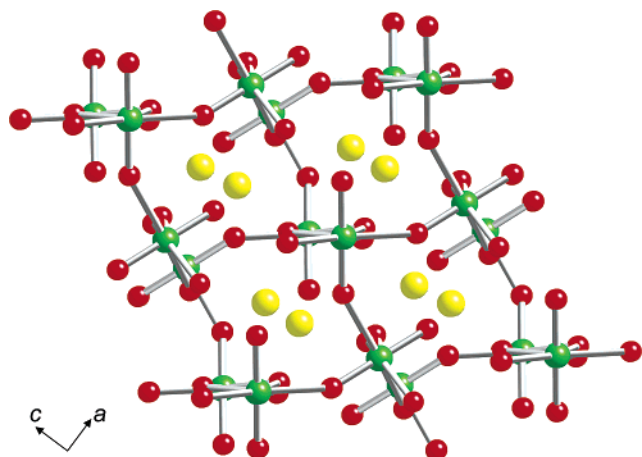


Figure 2. Stacking arrangement of the three-dimensional structure of $\text{Na}[\text{NpO}_2(\text{OH})_2]$ viewed down the b -axis along chain growth. The one-dimensional chain substructure is fused together through a network of cation-cation interactions that run along the ac direction. Sodium cations (yellow) reside in the channels.

Np cation. It is part of a nearly linear NpO_2^+ neptunyl ion with bond lengths of 1.895(3) and 1.879(3) Å, which are somewhat longer than are typical for $\text{Np}(\text{V})=\text{O}$ bonds. The neptunyl ion is coordinated by four OH groups and one O atom that are arranged at the equatorial vertices of a pentagonal bipyramid. The structure contains a single Na site that is coordinated by three OH groups and three O atoms of neptunyl ions, with bond lengths ranging from 2.315(4) to 2.811(4) Å.

The $(\text{NpO}_2)\text{O}(\text{OH})_4$ pentagonal bipyramids share an edge defined by two hydroxyl groups, resulting in a chain that is one bipyramid wide (Figure 1). Topologically identical chains of uranyl pentagonal bipyramids are known from moctezumite, $[\text{PbUO}_2(\text{TeO}_3)_2]$,²⁷ and $(\text{UO}_2)\text{Cl}_2(\text{H}_2\text{O})$.²⁸ Each chain extends along the b -axis and is rotated by approximately 60° relative to neighboring chains. The relative orientations of the chains facilitate cation-cation interactions between the chains, in which the O3 atom of each neptunyl ion is also an equatorial ligand of a pentagonal bipyramid of an adjacent chain (Figure 2). The cation-cation interactions link the chains into a three-dimensional network (Figure 3).

A bond-valence sum calculation for $\text{Np}(\text{V})$ gave 4.78.²⁰ The five equatorial $\text{Np}-\text{O}$ bond lengths range from 2.377(3) to 2.470(3) Å, with O(3') involved in the cation-

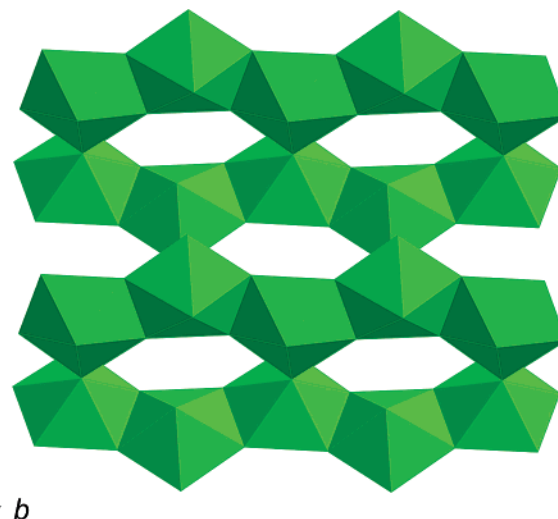


Figure 3. View along the a -axis depicting the chains from Figure 1 linked through cation-cation interactions to form small channels void of sodium cations.

Table 2. Selected Bond Lengths (angstrom) and Angles (deg) for $\text{Na}[\text{NpO}_2(\text{OH})_2]$ (1)

$\text{Np}(1)-\text{OH}(1)$	2.437(3)
$\text{Np}(1)-\text{OH}(1)^a$	2.406(3)
$\text{Np}(1)-\text{OH}(2)$	2.405(3)
$\text{Np}(1)-\text{OH}(2)^b$	2.377(3)
$\text{Np}(1)=\text{O}(3)$	1.895(3)
$\text{Np}(1)-\text{O}(3)^c$	2.470(3)
$\text{Np}(1)=\text{O}(4)$	1.879(3)
$\text{O}(3)=\text{Np}(1)=\text{O}(4)$	179.6(1)
$\text{Np}(1)-\text{O}(1)-\text{Np}(1)^a$	110.71(1)
$\text{Np}(1)=\text{O}(2)=\text{Np}(1)^b$	112.86(1)
$\text{Np}(1)=\text{O}(3)=\text{Np}(1)$	150.47(2)

^{a-c}Symmetry transformations used to generate equivalent atoms: (a) $-x, y - 1/2, -z + 3/2$; (b) $-x, y + 1/2, -z + 3/2$; (c) $x + 1/2, -y + 1/2, -z + 1$.

cation interaction being the longest. The distance between Np within the chain is 3.9843(2) Å, whereas the shortest Np-Np interchain distance and corresponding to a cation-cation interaction is 4.2232(2) Å. Na^+ cations reside in channels (Figure 2) that extend along the b -axis. Small empty channels also extend along the a -axis (Figure 3). Selected bond distances and angles for **1** are given in Table 2.

The structure of **1** adopts a topology that is unlike those of uranyl oxide hydrate phases (Table 3). To date there are 34 uranyl oxide hydrate structures, of which 22 are minerals. With the exception of $\text{Pb}_2(\text{H}_2\text{O})[(\text{UO}_2)_{10}\text{UO}_{12}(\text{OH})_6(\text{H}_2\text{O})_2]$ ²⁹ and $(\text{NH}_4)_3(\text{H}_2\text{O})_2[(\text{UO}_2)_{10}\text{O}_{10}(\text{OH})][(\text{UO}_4)(\text{H}_2\text{O})_2]$,¹⁸ all are based upon sheets of uranyl polyhedra with low-valence cations in the interlayers between the sheets. Seven of the 22 minerals and 3 of the 12 synthetic phases contain the well-known $\alpha\text{-U}_3\text{O}_8$ sheet-type that is based on the protasite anion topology.¹⁴ The sheets in these compounds are composed of edge-sharing uranyl pentagonal bipyramids and do not involve cation-cation interactions. It is evident from the range of chemistry accommodated by these structures that this sheet topology can accommodate a variety of interlayer cations and hydroxyl anion distributions. In addition to phases containing the $\alpha\text{-U}_3\text{O}_8$ -type sheet, many other uranyl oxide hydrates are based upon topologically

(27) Swihart, G. H.; Sen Gupta, P. K.; Schlemper, E. O.; Back, M. E.; Gaines, R. V. *Am. Mineral.* **1993**, *78*, 835-839.

(28) Taylor, J. C.; Wilson, P. W. *Acta Crystallogr., Sect. B* **1974**, *30*, 169-175.

(29) Li, Y.; Burns, P. C. *Can. Mineral.* **2000**, *38*, 727-735.

Table 3. Atomic Coordinates and Equivalent Isotropic Displacement Parameters for Na[NpO₂(OH)₂] (1)

atom	x	y	z	U_{eq} (Å ²) ^a
Np(1)	0.0382(1)	0.2359(1)	0.6851(1)	0.008(1)
Na(1)	0.5038(4)	0.4722(3)	0.8327(3)	0.030(1)
OH(1)	0.1434(7)	0.5383(4)	0.6260(4)	0.018(1)
OH(2)	0.0888(6)	-0.0663(4)	0.6093(4)	0.015(1)
O(3)	-0.2410(5)	0.2626(4)	0.5723(4)	0.017(1)
O(4)	0.3136(6)	0.2091(4)	0.7988(3)	0.015(1)

^a U_{eq} is defined as one-third of the trace of the orthogonalized U_{ij} tensor.

diverse sheets of uranyl square and pentagonal bipyramids. Some of these are extraordinarily complex, such as the sheet in the mineral wölsendorfite, Pb_{6.16}Ba_{0.36}[(UO₂)₁₄O₁₉(OH)₄](H₂O)₁₂, which has a primitive repeat distance of approximately 56 Å.³⁰

Pb₂(H₂O)[(UO₂)₁₀UO₁₂(OH)₆(H₂O)₂] and (NH₄)₃(H₂O)₂[(UO₂)₁₀O₁₀(OH)][UO₄](H₂O)₂] are exceptional uranyl(VI) oxide hydrates because they possess framework structures. Pb₂(H₂O)[(UO₂)₁₀UO₁₂(OH)₆(H₂O)₂] has a framework created from two-dimensional slabs that are related to the curite-type sheet³¹ are in turn linked by U(VI)O₆ octahedra. Covalent bonding occurs between opposing oxo groups of these UO₆ moieties and other uranyl(VI) sites within the sheets, but these are not considered cation–cation interactions because the coordination environment about these U⁶⁺ cations are distorted octahedra, rather than uranyl-containing polyhedra. This is evidenced by elongation of the U–O bonds relative to typical uranyl U=O distances of approximately 1.8 Å to approximately 2.03 Å. (NH₄)₃(H₂O)₂[(UO₂)₁₀O₁₀(OH)][UO₄](H₂O)₂] also possesses a three-dimensional structure. It contains two-dimensional sheets of pentagonal bipyramids with the α-U₃O₈ sheet topology. The sheets are cross-linked by uranyl polyhedra in which the uranyl ions are approximately parallel to the sheets, through cation–cation interactions.¹⁸ Such UO₂²⁺–UO₂²⁺ cation–cation interactions are rare and only occur in approximately 2% of all known U(VI) structures.^{14,17}

The three-dimensional structure of **1** departs dramatically from the well-known two-dimensional sheet topologies common for uranyl oxide hydrates, mostly owing to the presence of cation–cation interactions. Conversely, neptunyl(VI), with the same charge and propensity to form a terminal actinyl unit as uranyl(VI), would be expected to form structures that are similar to those common for uranium. Two-dimensional structures dominate hexavalent uranium crystal chemistry, and typically three-dimensional compounds are only formed by the linkage of uranyl polyhedra with uranyl ions parallel to the sheets or by the incorporation of oxo anions such as silicate to cross-link sheet topologies into a framework. Several neptunyl(V) compounds form three-dimensional networks and involve cation–cation interactions, including NpO₂HCOO³² and (NpO₂)₂SO₄·2H₂O.³³ Some of the two-dimensional sheet topologies observed also contain

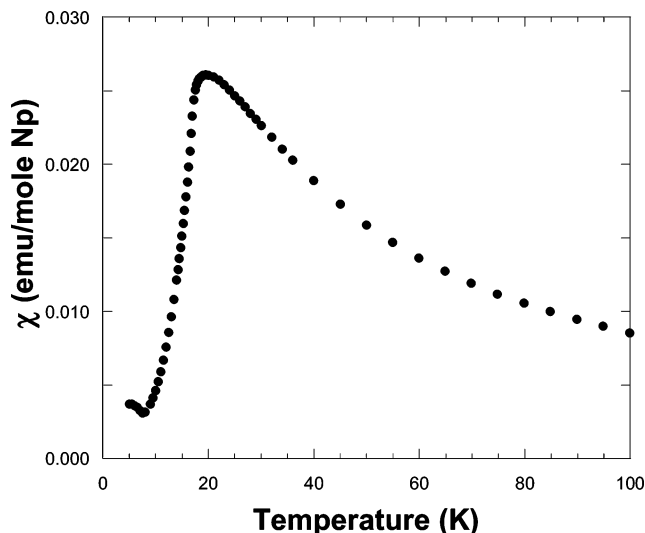


Figure 4. Magnetic susceptibility of Na[NpO₂(OH)₂] obtained under an applied field of 500 G. The data show a cusp at 19.5(5) K in the magnetic response that is consistent with an antiferromagnetic ordering of the Np⁵⁺ magnetic moments.

cation–cation interactions, such as La(NpO₂)₃(NO₃)₆·nH₂O,³⁴ [(NpO₂)₂SO₄(H₂O)],^{35,36} and [(NpO₂)₂CH₂(COO)₂(H₂O)₃]·H₂O,³⁷ as well as one-dimensional chain and ribbon topologies observed in NpO₂ClO₄(H₂O)₄,³⁸ (NpO₂)₂(NO₃)₂(H₂O)₄·H₂O,³⁹ and NaK₃(NpO₂)₄(SO₄)₄(H₂O)₂.⁷ Cation–cation interactions can facilitate frameworks perhaps unattainable for uranyl structures.

Magnetic Properties. The magnetic susceptibility data were obtained on three different samples and are represented by those obtained from a 3.6 mg polycrystalline sample over the temperature range of 5–320 K and under an applied field of 500 G. The data, shown in Figure 4, reveal a cusp at 19.5(5) K that is characteristic of antiferromagnetic ordering below that temperature. A comparison of zero-field cooled and field cooled susceptibilities below the transition (not shown) indicates that there may be a small ferromagnetic component to the magnetism or that there is a small ferromagnetic impurity. The magnitude of the ferromagnetic response changes with synthetic batch, but even in the worst case, and assuming a 1 μ_B moment, any impurity phase is estimated to comprise no more than 0.1% of the sample. All observable peaks in powder diffraction patterns obtained from the magnetism samples are indexable in the space group of the parent compound, P2₁2₁2₁.

The data are consistent with antiferromagnetically coupled Np magnetic moments below 19.5 K. The parent space group contains only one Np per asymmetric unit, and therefore all Np share the same energy-level scheme, magnetic moment, and exchange pathways, which serves to limit the possible

(30) Burns, P. C. *Am. Mineral.* **1999**, *84*, 1661–1673.

(31) Li, Y.; Burns, P. C. *Can. Mineral.* **2000**, *38*, 1433–1441.

(32) Grigor'ev, M. S.; Yanovskii, A. I.; Struchkov, Y. T.; Bessonov, A. A.; Afonasyeva, T. V.; Krot, N. N. *Radiokhimiya* **1989**, *31*, 37–44.

(33) Grigor'ev, M. S.; Yanovskii, A. I.; Fedoseev, A. M.; Budantseva, N. A.; Struchkov, Y. T.; Krot, N. N.; Spitsyn, V. I. *Dokl. Akad. Nauk SSSR* **1988**, *300*, 618–622.

(34) Grigor'ev, M. S.; Charushnikova, I. A.; Krot, N. N. *Radiochemistry (New York)* **2005**, *47*, 549–551.

(35) Grigor'ev, M. S.; Baturin, N. A.; Budantseva, N. A.; Fedoseev, A. M. *Radiokhimiya* **1993**, *35*, 29–38.

(36) Forbes, T. Z.; Burns, P. C.; Soderholm, L.; Skanthakumar, S. *Mater. Res. Soc. Proc.* **2006**, *893*, 375–380.

(37) Grigor'ev, M. S.; Charushnikova, I. A.; Krot, N. N.; Yanovskii, A. I.; Struchkov, Y. T. *Radiokhimiya* **1993**, *35*, 24–30.

(38) Grigor'ev, M. S.; Baturin, N. A.; Bessonov, A. A.; Krot, N. N. *Radiochemistry* **1995**, *37*, 12–14.

(39) Grigor'ev, M. S.; Charushnikova, I. A.; Krot, N. N.; Yanovskii, A. I.; Struchkov, Y. T. *Zh. Neorg. Khim.* **1994**, *39*, 179–183.

magnetic structures. Nevertheless because there are four Np/unit cell there are several possible coupling symmetries for the magnetic structure, which may be either consistent with the crystallographic unit cell or may result in larger unit cells. Neither a detailed description of the magnetic structure itself nor a quantitative determination of the saturation moment on the Np(V) can be obtained without neutron diffraction studies as a function of temperature.

An evaluation of the published data for Np(V) compounds reveals that the magnetic coupling is usually ferromagnetic and that the ordering temperatures are in the range of 8–12 K.^{7,20} The highest ordering temperature published to date for a neptunyl(V) compound, 12 K, is the ferromagnetic transition temperature for NpO₂(O₂CH)(H₂O), the structure of which includes 2D sheets of cation–cation interactions with an intersheet separation of 7.06 Å.²² The magnetic ordering reported herein for NaNpO₂(OH)₂ is the only example to date of antiferromagnetic ordering of Np(V) moments, and 19.5 K is the highest of the reported ordering temperatures for these compounds.

Insight into the simultaneous occurrence of antiferromagnetic coupling and an unusually high ordering temperature in **1** may be obtained by an examination of the structure. All neptunyl(V) compounds reported to date that exhibit magnetic ordering, for which the structures are known include cation–cation interactions. The cation–cation interactions, which provide a potential superexchange pathway, occur along the crystallographic *ac* direction, with a Np–Np distance of 4.2323 Å and Np–O–Np bond angle of 150.6°, within the range reported for these interactions.¹⁵ In addition to the Np–Np linkages through cation–cation interaction, the structure also contains Np–(OH)₂–Np linkages, shown in Figure 1, that extend perpendicular to the cation–cation interactions, as chains along the *b*-direction, resulting in short Np–Np distances of 3.9834 Å and Np–O–Np bond angles of 110.3° and 112.7°. Although the Np–Np distance along the chain is within the range of distances seen for cation–cation interactions, the Np–(OH)₂–Np bond angle is significantly reduced, more closely associated with a 90° than a 180° superexchange pathway.⁴⁰ The very different Np–O–Np bond angles associated with the dihydroxybridged interactions implies very different orbital symmetry for the two superexchange pathways that could influence the net magnetic interaction strength, depending on the detailed symmetry of the occupied and low-lying hybridized Np(V) crystal-field states. For the hydroxide under discussion herein, this complex bonding appears to enhance antiferromagnetic over ferromagnetic interactions and to result in a higher ordering temperature. This complex structure may explain, in part, the occurrence of a variable ferromagnetic component of the ordered magnetic response.

The magnetic response above the ordering temperature is shown in Figure 5. The data were fit using a modified Curie–Weiss law $\chi(T) = C/(T - \theta) + \chi_{\text{TIP}}$, in which *C* is the Curie constant, from which the effective magnetic moment can be derived, $\mu_{\text{eff}} = [3kC/N]^{1/2}$; θ is the Weiss constant, a

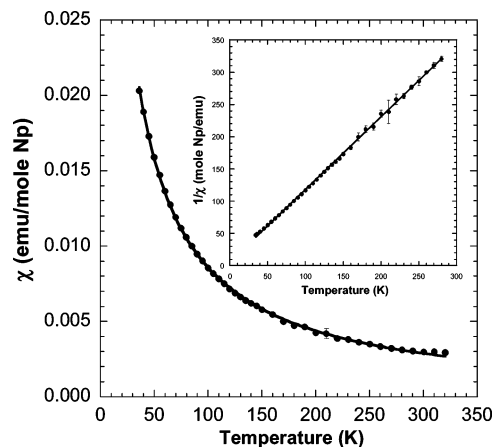


Figure 5. Magnetic susceptibility of Na[NpO₂(OH)₂] from 35 to 320 K, above the magnetic ordering temperature, together with the best fit (solid line), as described in the text. Inset: the same data presented as a Curie–Weiss plot, which was used to obtain the effective moment, 2.80(15) μ_{B} , and the Weiss constant, –10 K.

temperature calibrant that may adjust for magnetic ordering, and a temperature-independent (TIP) contribution, which may result from either conduction electrons or second-order crystal-field contributions. A fit to the data reveals an effective moment of 2.82(2) μ_{B} per Np, a Weiss constant of –12(5) K, and a negligible temperature-independent contribution. A plot of the inverse susceptibility versus temperature, which assumes the classic Curie–Weiss behavior, is linear and thus confirms the negligible TIP contribution to the data.⁷ A fit to the inverse susceptibility versus temperature data results in an effective moment of 2.80(15) μ_{B} per Np and a Weiss constant of –10(4) K, in agreement with the full fit.

The effective moment determined here for **1** is significantly less than the free ion value of 3.58 μ_{B} expected for an *f*² configuration in a Russell–Saunders coupling scheme. Reduced moments have also been reported for the trihydrate of NpO₂(O₂C₂)₂C₆H₄(H₂O)₃, with an effective moment of 2.54 μ_{B} , and NpO₂(O₂CH)(H₂O), with a value of 2.83 μ_{B} . The effective moments reported for Np(V) compounds vary considerably, likely the result of detailed differences in crystal-field splitting of the ³H₄ ground term.⁴¹ Whereas a detailed analysis of the effect of the crystal-field on the ground term has not been published for NpO₂⁺, such studies have been done for Pr³⁺, which also has an *f*² configuration.^{42,43} The ground Γ_5 state has an effective moment of 2.8 μ_{B} . Although NpO₂⁺ has the same configuration to first order, the change from 4*f* to 5*f* electrons has several important implications. Most important are the expectations of enhanced configuration mixing for the 5*f* electrons and the increased importance of *j*–*j* coupling, along with the increased size of the crystal-field splitting relative to the spin–orbit interaction.⁴⁴ In addition to these considerations, the dioxo ligation results in a very strong axial electric field

(40) White, R. M. *Quantum Theory of Magnetism*, 2nd ed.; Springer-Verlag: Berlin, 1983.

(41) Nakamoto, T.; Massami, N.; Nakamura, A. *Recent Res. Dev. Inorg. Chem.* **2000**, 2, 145–163.

(42) Lea, K. R.; Leask, J. M.; Wolf, W. P. *J. Phys. Chem. Solids* **1962**, 23, 1381–1405.

(43) Staub, U.; Soderholm, L. In *Handbook on the Physics and Chemistry of Rare Earths*; Gschneidner, K. A., Jr., Eyring, L., Maple, M. B., Eds.; Elsevier Science BV: Amsterdam, 2000; Vol. 30, pp 491–545.

(44) Carnall, W. T. *J. Chem. Phys.* **1992**, 96, 8713–8726.

at the Np⁵⁺ site that will further split the crystal-field states. A combination of these factors could result in the small effective moment observed for selected neptunyl(V) compounds. Further studies are required before a systematic picture of the magnetic properties of these novel compounds will emerge.

Acknowledgment. This research was funded by the National Science Foundation Environmental Molecular Science Institute

at the University of Notre Dame (EAR02-21966) and at Argonne by the DOE, OBES—Chemical Sciences, under contract W-31-109-ENG-38.

Supporting Information Available: X-ray crystallographic files (CIF), atomic coordinates, and equivalent isotropic displacement parameters for Na[NpO₂(OH)₂]. This material is available free of charge via the Internet at <http://pubs.acs.org>.

CM0621040